

Loss of *Lkb1* cooperates with *Braf*^{V600E} and ultraviolet radiation, increasing melanoma multiplicity and neural-like dedifferentiation

Kimberley McGrail¹, Elena González-Sánchez^{1†}, Paula Granado-Martínez¹, Roberto Orsenigo¹, Yuxin Ding¹, Berta Ferrer², Javier Hernández-Losa², Iván Ortega^{3‡}, Juan Martín-Caballero^{3§}, Eva Muñoz-Couselo⁴, Vicente García-Patos⁵ and Juan A. Recio¹ (1)

- 1 Biomedical Research in Melanoma-Animal Models and Cancer Laboratory, Vall d'Hebron Research Institute VHIR, Vall d'Hebron Hospital-UAB, Barcelona, Spain
- 2 Anatomy Pathology Department, Vall d'Hebron Hospital-UAB, Barcelona, Spain
- 3 Animal Laboratory Unit, Biomedical Research Park of Barcelona-PRBB, Spain
- 4 Clinical Oncology Program, Vall d'Hebron Institute of Oncology (VHIO), Vall d'Hebron Hospital-UAB, Barcelona, Spain
- 5 Dermatology Department, Vall d'Hebron Hospital-UAB, Barcelona, Spain

Kevwords

BRAF^{V600E}; LKB1; melanoma; neural crest like; ultraviolet radiation

Correspondence

J. A. Recio, Biomedical Research in Melanoma, Animal Models and Cancer Laboratory, Vall d'Hebron Research Institute VHIR, Vall d'Hebron Hospital-UAB, Barcelona 08035, Spain E-mail: juan.recio@vhir.org

Present address

†Miltenyi Biotec S.L., Madrid, Spain ‡University of Barcelona, Bellvitge, Spain §Instituto Cajal, Consejo Superior de Investigaciones Científicas (CSIC), Madrid, Spain

(Received 11 June 2024, revised 4 July 2024, accepted 26 July 2024)

doi:10.1002/1878-0261.13715

The mechanisms that work alongside $BRAF^{V600E}$ oncogene in melanoma development, in addition to ultraviolet (UV) radiation (UVR), are of great interest. Analysis of human melanoma tumors [data from The Cancer Genome Atlas (TCGA)] revealed that 50% or more of the samples expressed no or low amounts of serine/threonine protein kinase STK11 (also known as LKB1) protein. Here, we report that, in a mouse model, concomitant neonatal Braf^{V600E} activation and Lkb1 tumor suppressor ablation in melanocytes led to full melanoma development. A single postnatal dose of UVB radiation had no effect on melanoma onset in Lkb1depleted mice compared with Braf^{V600E}-irradiated mice, but increased tumor multiplicity. In concordance with these findings and previous reports, Lkb1-null irradiated mice exhibited deficient DNA damage repair (DDR). Histologically, tumors lacking Lkb1 were enriched in neural-like tumor morphology. Genetic profiling and gene set enrichment analyses of tumor sample mutated genes indicated that loss of Lkb1 promoted the selection of altered genes associated with neural differentiation processes. Thus, these results suggest that the loss of Lkb1 cooperates with Braf^{V600E} and UVR, impairing the DDR and increasing melanoma multiplicity and neural-like dedifferentiation.

Abbreviations

4EBP1, eukaryotic translation initiation factor 4E-binding protein 1; 4OHT, 4-hydroxytamoxifen; 6-4pps, pyrimidine (6–4) pyrimidone photoproducts; AKT, serine/threonine-protein kinase Akt; *B, Braf*^{CA} mouse model; *B;L, Braf*^{CA+}; *Lkb1*^{-/-} mouse model; BRAF, serine/threonine-protein kinase B-raf; CPD, cyclobutane pyrimidine dimer; DAB, 3,3-diaminobenzidine tetrahydrochloride; DDR, DNA damage response; DMBA, 7,12-dimethylbenz[α]anthracene; ERK, extracellular signal-regulated kinase; FFPE, formalin-fixed paraffin embedded; IHC, immunohistochemistry; LKB1, liver kinase B1 homolog; MAPK, mitogen-activated protein kinase; MEK, meiosis-specific serine/threonine protein kinase; mTORC1, mammalian target of rapamycin complex 1; mTORC2, mammalian target of rapamycin complex 2; NF1, neurofibromin; OIS, oncogene-induced senescence; PJS, Peutz–Jeghers syndrome; PTEN, phosphatidylinositol 3,4,5-trisphosphate 3-phosphatase and dual-specificity protein phosphatase; RAF, RAF proto-oncogenes serine/threonine protein kinase; RAS, GTPase RAS; S6, ribosomal protein S6; STK11, serine/threonine protein kinase STK11; TCGA, The Cancer Genome Atlas; TMB, tumor mutational burden; TRP2, L-dopachrome tautomerase; UV, ultraviolet; UVB, ultraviolet radiation type B; UVR, ultraviolet radiation; VAF, variant allele frequency.

1. Introduction

Cutaneous melanoma is the most aggressive form of skin cancer and is responsible for the majority of skin cancer-related deaths. In melanoma, BRAF mutation is the most frequent alteration (50% of melanoma tumors) leading to abnormal activation of the RAS/-RAF/MEK/ERK signaling pathway [1-3]. There are no differences in the frequency of BRAF mutations between benign and tumoral lesions [4], indicating that mutated BRAF is not sufficient for melanoma transformation [5]. Multiple studies have identified major host and environmental risk factors for melanoma. The predominant environmental risk factor is exposure to UV radiation (UVR), which is responsible for the generation of DNA mutations that, if not properly repaired, can result in genomic instability and, consequently, tumorigenesis [6,7]. The cooperation of UVR and BRAF mutations in promoting malignant melanoma has been previously described in different contexts [8,9]. In addition to UVR, the expression of BRAF V600E combined with the silencing of the tumor suppressor PTEN [10] or the downregulation of the tumor suppressor NF1 [11] induces melanoma development and progression.

Serine threonine kinase 11 (STK11), also known as LKB1, is a ubiquitously expressed and evolutionarily conserved serine/threonine kinase identified as a tumor suppressor. It is involved in a number of biological processes, including DDR [12-15]. LKB1 has been found to be mutated in several tumor types, such as lung cancer [16,17], cervical cancer [18], pancreatic cancer [19,20], breast cancer [21], and malignant melanoma [22,23]. In fact, Peutz-Jeghers syndrome (PJS), which results from germline mutations in LKB1, is characterized by an increased probability of developing cancer [24,25]. Several studies have shown that cancer development and progression can be promoted in the absence of LKB1 even in haploinsufficiency conditions [12]. In the case of melanoma, Lkb1 inactivation facilitates the expansion of pro-metastatic melanoma cell subpopulations upon RAS pathway activation [26]. In addition, LKB1 inactivation synergized with $BRAF^{V600E}$, promoting cell transformation [27]. Moredeficiency Lkb1sensitized DMBA-induced skin and lung squamous cell carcinomas [28] and increased the progression of lung adenomas to carcinomas [29]. Additionally, LKB1 plays a crucial role in the regulation of neural crest cell migration and differentiation during embryonic development, where dysregulation of LKB1 function can lead to defects in neural crest cell development and contribute to various developmental abnormalities [30].

Melanoma tumors are characterized by a high mutational burden resulting from exposure to UVR. LKB1 loss contributes to tumor development and progression in several tumor types, including BRAF-mutant melanoma, under different genetic conditions. Given that LKB1 plays a relevant role in DDR [12] and neural crest cell differentiation [30], we investigated the contributions of Lkb1 loss to UVR-induced melanoma development and progression in a BrafV600E-mutant animal model. Our data show that a substantial fraction of BRAF-mutated human melanomas either do not express or express low amounts of LKB1. In vivo modeling of UV-induced Braf V600E-mutated melanoma showed that loss of Lkb1 cooperated with Braf V600E and UVR, impairing DDR and increasing melanoma multiplicity and dedifferentiation.

2. Materials and methods

2.1. Mouse model

All mice were cared for and maintained in accordance with animal welfare regulations under an approved protocol by the Institutional Animal Care and Use Committee at Vall d'Hebron Institut de Recerca (VHIR) and Biomedical Research Park of Barcelona (PRBB). Braf^{CA/CA} strain has been previously described [10,31]. Tyr::Cre^{ERT2}; Lkb1^{flox/flox} mice were obtained from Marcus Bosenberg (Yale University, New Heaven, USA). Original Tyr::CreERT2 mice were from Lynda Chin (Dana Farber, Boston, USA). We crossed the Tyr::CreERT2; Lkb1flox/flox strain with Braf^{CA/CA} mice and generated their Mendelian offspring in a mixed genetic background. The Tyr:: Cre^{ERT2} ; $Brat^{CA/CA}$; $Lkb1^{F/F}$ strain was previously described [29]. Both sexes were used for the experiments. All animals were housed and cared for in an SPF-grade animal facility, under the supervision of the Biomedical Research Park of Barcelona (Prbb) specialized animal facility personnel. All the experiments and studies were performed according to a protocol approved by the Institutional Animal Care and Use Committee at Biomedical Research Park of Barcelona (Prbb) (CEEA: JMC-10-1309P2).

2.1.1. Melanoma development in vivo

Mice were treated topically on postnatal Days 2.5 and 3.5 with 100 μ L of an acetone solution containing 5 mg·mL⁻¹ 4-hydroxytamoxifen (4OHT) (Sigma, St. Louis, MO, USA). Neonatal mice were irradiated on

postnatal Day 3.5 as previously described [32]. Tumor development data were analyzed by Kaplan–Meier survival analysis.

2.2. Human melanoma samples

All pseudonymized human melanoma tissue samples were provided by the Vall d'Hebron Research Hospital under the National Research Ethics Service approved study number PR(AG)59-2009. All study methodologies conformed to the standards set by the Declaration of Helsinki. A written informed consent was provided by all patients.

2.3. Immunohistochemistry (IHC)

4 μm sections of formalin-fixed paraffin-embedded skin or tumor samples were stained following the manufacturer's protocol. The samples were developed by using either secondary antibodies linked to horseradish peroxidase with the UltraViewTM Universal DAB Detection Kit (Ventana Medical System; Roche, Tucson, AZ, USA) or secondary antibodies linked to fluorophores. Staining was performed either manually or using the automated immunostainer Beckmarck XT (Ventana Medical Systems). For the samples processed manually, antigen retrieval was performed using a target retrieval solution at pH 6.0 or pH 9.0 according to antibody protocol recommendations (Agilent, Santa Clara, CA, USA). The samples were scanned (panoramic slide digital scanner) and evaluated by two independent pathologists (using 3DHistech Software: Budapest, Öv u. 3., Hungary). LKB1 (#13031; 1:250), p-AKT^{S473} (#4060; 1:100), $p-S6^{S235/236}$ (#2211; 1:500), and $p-4EBP1^{T37/46}$ (#2855; 1:1000) antibodies were obtained from Cell Signaling (Danvers, MA, USA). A Cre antibody (NB100-56135; 1:1000) was obtained from Novus Biologicals (Littleton, CO, USA). BRAF^{V600E} (#760-5095) was purchased from Ventana Medical System. TRP2 (Dct, Pep8) was obtained from V. Hearing (National Institute of Health) [33]. Secondary fluorescent antibodies were purchased from Thermo Fisher Scientific (Waltham, MA, USA). For H-score evaluation, the samples were scanned (panoramic slide digital scanner) and evaluated by two independent pathologists (using 3DHistech software). The H-score was calculated according to the following formula: H-score = [(0 × % negative cells) + (1 × % weak positive cells) + $(2 \times \%$ moderate positive cells) + $(3 \times \% \text{ strong positive cells})$, with the overall score ranging from 0 (negative) to 300 (100% strong staining).

2.4. Dot blot

The back skins of the $Tvr::Cre^{ERT2}$; $Braf^{CA/CA}$; $Lkb1^{F/F}$ untreated and 4OHT-treated 2.5-day-old neonates were collected 20 h and 7 days after treatment with UVR. Genomic DNA was isolated using a DNeasy kit (Qiagen, Venlo, the Netherlands) following the manufacturer's recommendations. A total of 100 ng of DNA was resuspended in 0.5 M NaOH and 10 mm EDTA, denatured, and spotted on a nitrocellulose membrane using Bio-Dot SF (Bio-Rad, Hercules, CA, USA). Then, the membrane was heated at 80 °C for 2 h and incubated with primary antibodies against 6-4 photoproducts (6-4 pps), Dewar photoproducts (Dewar pps), and cyclobutane pyrimidine dimers (CPDs), which were purchased from CosmioBio (Carlsbad, CA, USA). Secondary antibodies were obtained from GE Healthcare (Chicago, IL, USA). Bound antibodies were detected by enhanced chemiluminescence (ECL) (GE Healthcare). DNA loading was assessed by reprobing the membrane with radiolabeled mouse genomic DNA with ethidium bromide (Sigma). Quantification of the spots was performed using IMAGEJ 1.53a (NIH, Bethesda, MD, USA).

2.5. Whole-exome sequencing

Whole-exome sequencing (WES) and data analysis were performed at the Genomic Facility of VHIO (Vall d'Hebron Oncology Institute). In brief, DNA genomic libraries were prepared from fresh tissue (tumor and nontumor) and FFPE tumor tissue DNA prior to exome capture (SureSelect XT Mouse All Exon; Agilent). Libraries were sequenced on a HiSeq2000 instrument (Illumina, San Diego, CA, USA) with a mean coverage of $100 \times$. Reads were aligned, and somatic variants were identified by comparison with nontumor samples (VarScan2).

2.6. Statistics

Statistical analyses were performed in GRAPHPAD PRISM 9.0 (GraphPad Software Inc., Boston, MA, USA) using a two-tailed Student's *t* test and Wilcoxon test to compare differences between two groups.

3. Results

3.1. A substantial fraction of *BRAF*^{V600E}-mutant human melanomas do not express LKB1

Loss of PTEN and NFI tumor suppressors, as well as UVR, cooperates with $BRAF^{V600E}$ in melanoma development and progression [10,11]. In the case of

Lkb1, it was suggested that its inactivation abrogated $Braf^{V600E}$ -induced cell growth arrest [27]. Furthermore, loss of Lkb1 impaired UV-induced DDR, leading to genetic instability and the development of skin tumors [12]. To further analyze the role of the tumor suppressor LKB1 in melanomas harboring the BRAF^{V600E} mutation, we analyzed the expression and mutational status of LKB1 in 448 human samples obtained from the TCGA database (Skin Cutaneous Melanoma; TCGA, PanCancer Atlas). The data analysis showed a tendency for a negative correlation between LKB1 (STK11) and BRAF mRNA expression, where the absolute number of LKB1 transcripts was greater than that of BRAF mRNA (Fig. 1A). In contrast, most of the tumors, including BRAF-mutated samples. expressed low amounts of LKB1, while the BRAF protein was highly expressed (Fig. 1A). The correlation between the respective amounts of LKB1 or BRAF mRNA and protein supported this observation (Fig. 1B). Similarly, analysis of the putative copy numbers of the LKB1 and BRAF genes revealed that LKB1 genetic modifications were related to shallow deletions, while BRAF genetic alterations principally corresponded to gains and amplifications, including BRAF mutations (Fig. 1C). We validated these results by immunohistochemistry in an independent set of human samples (14 human BRAF^{V600E}-mutated melanomas). H-score quantification of the samples revealed that while 85% of the samples showed positive staining for BRAF^{V600E}, 42% of the samples showed either low or no expression of the LKB1 protein (Fig. 1D). Taken together, these results suggest that a substantial fraction of BRAF words mutated melanomas might exhibit LKB1-dependent functional impairments.

3.2. Neonatal loss of *Lkb1* cooperates with *Braf*^{V600E} in melanoma development and increases tumor multiplicity in UVR-induced melanoma

Epidemiological studies have demonstrated a strong association between UV radiation and melanoma

risk, where DNA is the major target of direct or indirect UV-induced cellular damage. Due to the role of LKB1 in the DDR [12] and the above observation suggesting the lack or low expression of LKB1 in BRAF^{V600E}mutant tumors, we investigated the contribution of Lkb1 loss to UVR-induced melanoma development and progression in a $Braf^{V600E}$ mutational context. To that end, we used conditional and inducible Tyr::CreERT2; Braf^{CA} mice [10]. Braf^{CA} mice express wild-type BRAF Cre-mediated to recombination 4OH-tamoxifen treatment, at which time oncogenic Braf V600E is expressed in physiological amounts. To generate the $Tyr::Cre^{ERT2};Braf^{CA};$ $Lkb1^{F/F}$ mouse, we crossed the $Tyr::Cre^{ERT2};Braf^{CA}$ mouse with the conditional knockout $Lkb1^{flox/flox}$ ($Lkb1^{F/F}$) mouse. As previously described, activation of BRAF did not promote melanoma development except in one old homozygous Braf^{CA/CA} mouse. However, UVB irradiation promoted melanoma development in 85.7% of Braf^{CA/+} and 87.5% of Braf^{CA/CA} mice. In contrast to previous reports [27], Lkb1 haploinsufficiency promoted melanoma development via the activation of either one Braf^{CA/+} allele (18.1%) or both Braf^{CA/CA} alleles (31.2%), albeit at late time points, as previously reported (mean onset times of 399 ± 38.9 and 285 ± 45 days, respectively). However, the loss of both Lkb1 alleles in mice harboring either one Braf-mutant allele (*Braf*^{CA/+}) or both *Braf*-mutant alleles (*Braf*^{CA/CA}) promoted a slight decrease in the incidence of melanoma, from 18.1% to 11% and from 31.2% to 12.5%, with an onset of 326 ± 90 and 319 ± 17 days, respectively (Fig. 2A). In comparison with that in UVRinduced melanomas, the tumor incidence in Braf^{CA/+} or Braf^{CA/CA} mice was not further increased upon Lkb1 loss (Fig. 2B). Nevertheless, the loss of the second Lkb1 allele promoted a slight delay in melanoma development together with an increase in tumor multiplicity (Fig. 2C, D). Overall, the above results showed that the loss of Lkb1 cooperates with Braf^{V600E} in melanocyte transformation, allowing melanoma development. Furthermore, loss of Lkb1 increased tumor multiplicity, particularly in response to UVR.

Fig. 1. Most BRAF^{V600E}-mutant human melanomas express low or no amounts of LKB1. (A) On the left, correlation between *BRAF* and *STK11* mRNAs in human melanoma samples. On the right, correlation between BRAF and LKB1 protein expression in human melanoma samples. The data were obtained from the cBioPortal database (Skin Cutaneous Melanoma; TCGA, PanCancer Atlas). (B) On the left, correlation between *STK11* mRNA expression and LKB1 protein expression. On the right, there was a correlation between the expression of *BRAF* mRNA and the expression of the BRAF protein. The data were obtained from the cBioPortal database (Skin Cutaneous Melanoma; TCGA, PanCancer Atlas). (C) Analysis of putative *STK11* and *BRAF* genomic copy numbers in relation to mRNA expression. The data were obtained from the cBioPortal database (Skin Cutaneous Melanoma; TCGA, PanCancer Atlas). Bars represent SD. (D) LKB1 immunostaining of BRAF^{V600E} human melanomas. Representative images of different tumor samples expressing low, medium, and high LKB1 levels are shown. On the right, a graphic representation of the LKB1 HScore against the BRAF^{V600E} HScore is shown. The scale bars correspond to 500 and 50 μm.

18780261, 0, Downloaded from https

onlinelibrary.wiley.com/doi/10.1002/1878-0261.13715 by Spanish Cochrane Nati

18780261, 0, Downloaded from https://febs.onlinelibrary.wiley.com/doi/10.1002/1878-0261.13715 by Spanish Cochrane National Provision

de Sanidad), Wiley Online Library on [30/01/2025]. See the Terms

on Wiley Online Library for rules of use; OA articles are governed by the applicable Creative Commons License

Fig. 2. Loss of Lkb1 cooperates with the $Brat^{VGOOE}$ mutation, promoting melanoma development. (A) Scheme of mouse treatments. Kaplan–Meier survival curve of mice treated with 4-hydroxytamoxifen (4OHTx) or 4OHTx + ultraviolet radiation (UVR). $Brat^{CA/+}$ (n = 18)/ $Brat^{CA/+}$; $Lkb1^{+/-}$ (n = 22)/ $Brat^{CA/+}$; $Lkb1^{-/-}$ (n = 18)/ $Brat^{CA/CA}$ (n = 17)/ $Brat^{CA/CA}$; $Lkb1^{+/-}$ (n = 16)/ $Brat^{CA/CA}$; $Lkb1^{-/-}$ (n = 16). (B) Table showing the total number of mice per group and the percentage of mice that developed melanoma tumors in response to either 4OHTx or 4OHTx + UVR treatments. P values for the calculated incidences are indicated. (C) Mean tumor onset and tumor multiplicity of $Brat^{CA/+}$ mice with or without one or both copies of Lkb1. The error bars represent the SDs. The P value was calculated by Willcoxon test. (D) Mean tumor onset and tumor multiplicity of $Brat^{CA/CA}$ mice with or without one or both copies of Lkb1. The error bars represent the SDs. The P value was calculated by Willcoxon test.

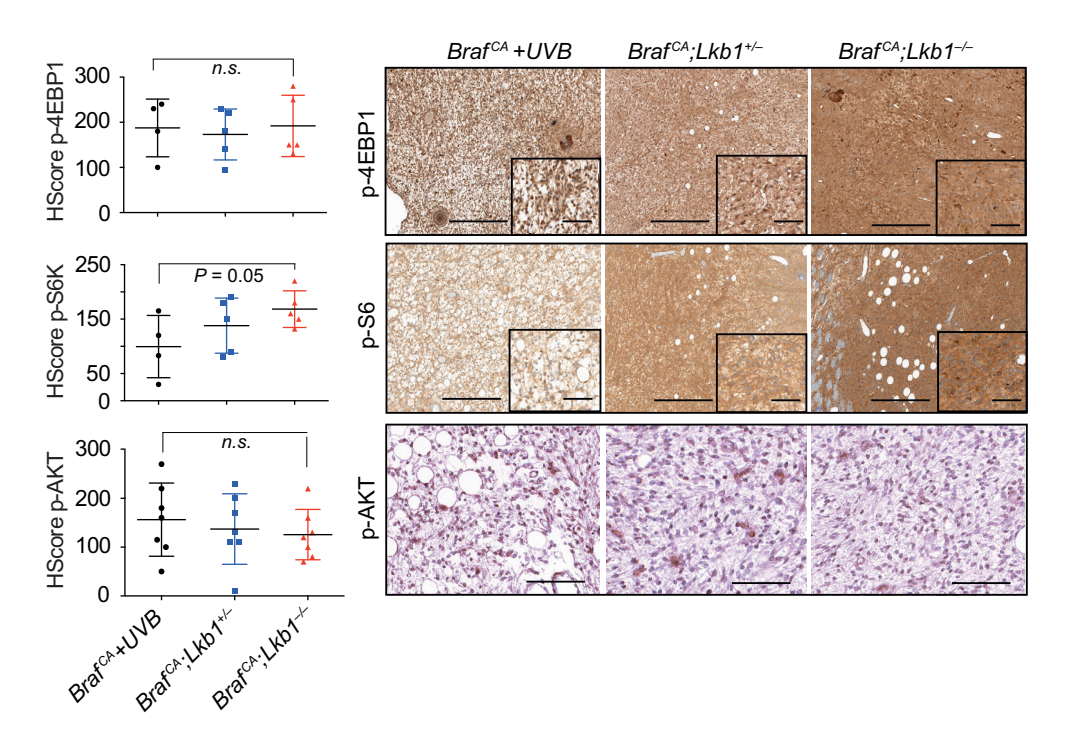


Fig. 3. Activation of both mTORC1 and mTORC2 is necessary for *Lkb1* loss-driven melanoma progression. Representative immunohistochemistry images of tumors from mice with the indicated genetic backgrounds showing p-4EBP1^{T37/46}, p-S6^{S235/236}, and p-AKT^{S473} staining. Graphs on the left show the HScore for these markers in seven different tumors from each genetic background \pm SD. The *P* value was calculated by Student's *t* test. The scale bars correspond to 500 μm.

3.3. UVR- and *Lkb1*^{F/F}-induced melanoma tumors showed activation of mTORC1/2

It has been previously described that in vivo Braf^{V600E}induced melanoma models require the concomitant activation of both mTORC1 and mTORC2/Akt for cell progression to malignancy [27]. The same study suggested that Lkb1 loss abrogated Braf^{V600E}-induced cell cycle arrest but did not lead to melanoma formation. Our data showed that the loss of *Lkb1* (even in haploinsufficiency) allowed the development of Braf V600E-mutant melanomas with a low incidence (11.1-31.2%) 10 months after Braf^{V600E} activation and Lkb1 knockout, most likely due to an increase in genomic instability. Since Lkb1 inactivation leads to mTORC1 activation, we investigated whether these tumors also acquired mTORC2 activation. Independent of the UV irradiation and Lkb1 status, all analyzed tumors stained positive for surrogate markers of mTORC1 activation, p-4EBP1^{T37/46}, p-S6^{S235/236}, and mTORC2-mediated phosphorylation of pAKT^{S473} (Fig. 3), suggesting the association of mTORC1/2 activation and Braf^{V600E}-driven melanoma. Thus, these results support that the loss of Lkb1 abrogates Braf^{V600E}-induced cell growth arrest, allowing malignant transformation over time and the activation of mTORC1/2.

3.4. Loss of *Lkb1* increases tumor heterogeneity and impairs UVR-induced DDR

As previously described [9,10,27], melanomas are mainly amelanotic, localized in the dermis or subcutaneous region, with no junctional component, and occasionally display several types of morphologies. We distinguished three major tumor morphologies: melanoma with myxoid features, spindle-shaped to round plump cell melanomas, and melanomas with neural differentiation (Fig. 4A). Braf^{V600E}-mutant tumors derived from UV radiation or Lkb1 loss were phenotypically heterogeneous (Fig. 4A); nevertheless, we could correlate the predominant type of lesions according to the mouse genotype and treatment (UVR). In absolute number, melanomas with myxoidlike morphology and spindle melanomas were predominant, and they developed mostly in response to UVR and independently of the absence of Lkb1. However, melanomas with neural differentiation were more frequent when Lkb1 was deleted, with or without UVR, suggesting the existence of tumor morphologies preferentially linked to Lkb1 dysfunction (Fig. 4B). We analyzed the frequency of different tumor morphologies according to the genetic dose of mutant Braf, alone or

18780261, 0, Downloaded from https://febs.onlinelibrary.wiley.com/doi/10.1002/1878-0261.13715 by Spanish Cochrane National Provision

de Sanidad), Wiley Online Library on [30/01/2025]. See the Terms

on Wiley Online Library for rules of use; OA articles are governed by the applicable Creative Commons License

in combination with the loss of one or both Lkb1 alleles. Overall, the loss of Lkb1 increased tumor heterogeneity. UV-independent myxoid-like melanomas were absent in either $Braf^{\mathrm{CA/+}}$; $Lkb1^{-/-}$ or $Braf^{\mathrm{CA/CA}}$; $Lkb1^{-/-}$ and UV-independent melanomas with neural

differentiation were mainly present in mice harboring the activation of two alleles of Braf (Braf $^{CA/CA}$) and the deletion of either one or both alleles of Lkb1 ($Lkb1^{+/-}$; $Lkb1^{-/-}$) (Fig. 4B). Due to the observed phenotypic heterogeneity of tumor cells and the

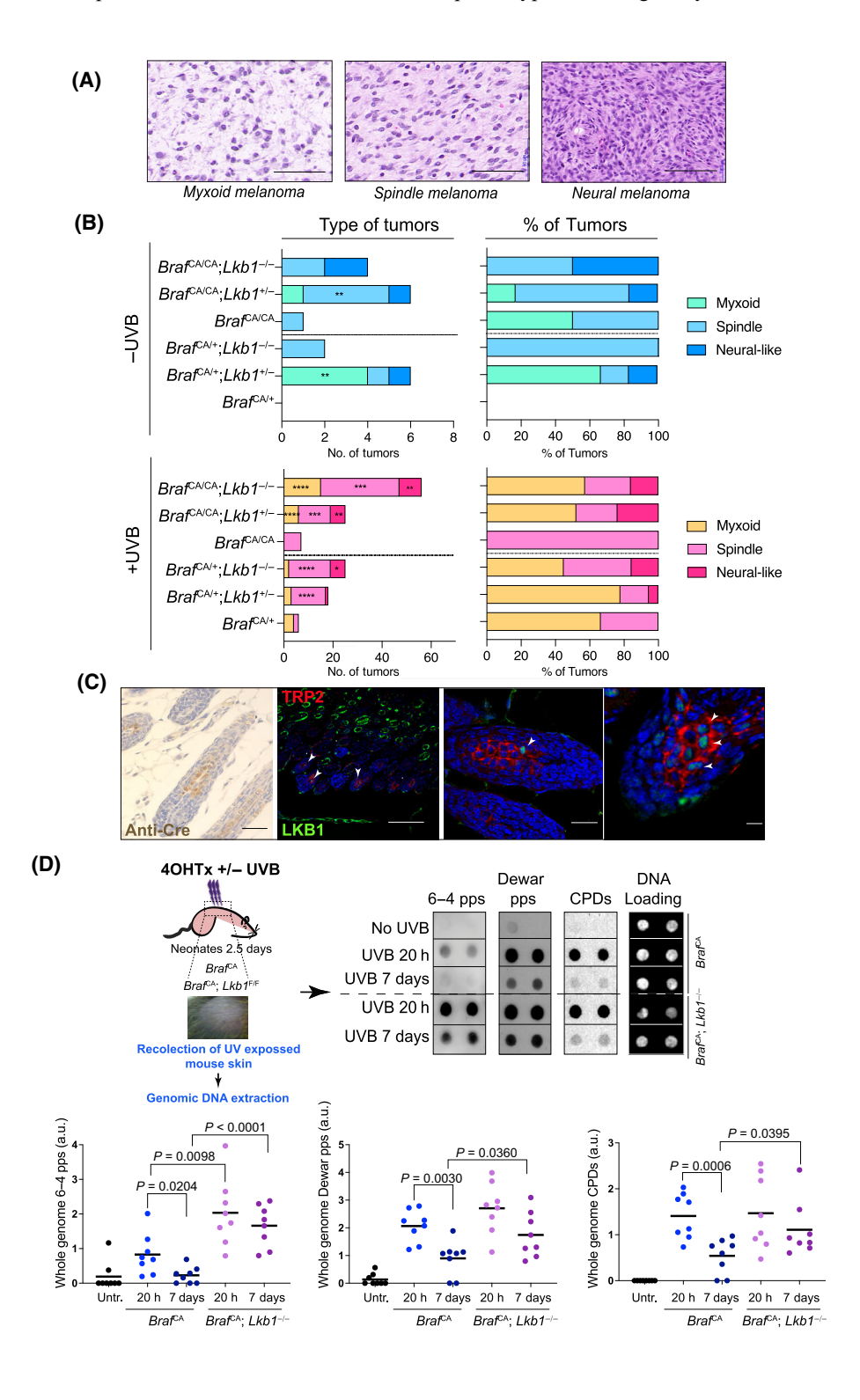


Fig. 4. Lkb1 loss promotes genomic instability and tumor heterogeneity. (A) Representative images of hematoxylin/eosin-stained tumors (n = 45 myxoid; n = 96 spindle; n = 32 neural-like) showing the histological melanoma subtypes. Bars represent 500 μm. (B) Graphs representing the number and percentage of the different melanoma subtypes according to the mouse genotype and the administered treatment. *P < 0.05; **P < 0.01; ***P < 0.001; ****P < 0.001. The P value was calculated by Student's t test comparing the values between genotypes according to the genetic dose in Braf. Number of mice per genotype and condition is indicated in Fig. 2B. In total, $Braf^{CA/CA}$; $Lkb1^{+/-}$ (n = 40); $Braf^{CA/CA}$; $Lkb1^{+/-}$ (n = 40); $Braf^{CA/CA}$; $Braf^{CA/CA}$; B

predominance of certain histological subtypes depending on the Lkb1 expression status, we analyzed the expression of LKB1 in mouse melanocytes. Interestingly, co-staining of normal mouse skin (7 days postnatal) for LKB1 and the melanocyte marker TRP2 revealed that only a small fraction of the mouse hair follicle melanocytes stained positive for LKB1 (Fig. 4C), suggesting a possible connection between tumor neural morphology and cellular origin. According to the data, the loss of Lkb1 increased tumor heterogeneity. Lkb1 loss impairs UVR-induced DDR, generating genetic instability. Thus, we analyzed the presence of UVB-induced DNA damage in mouse skin 20 and 7 days after UVB irradiation. The data revealed that 6-4 photoproducts (6-4 pps), Dewar derivatives, and cyclobutane pyrimidine dimers were still detected at high rates in Braf^{CA};Lkb1^{-/-} mice 7 days after UV irradiation, while they were almost completely repaired in wild-type mice (Fig. 4D), supporting the role of Lkb1 in the generation of genomic instability and consequently tumor heterogeneity.

3.5. Tumor genetic profiling revealed that *Lkb1* loss was associated with neural differentiation

To obtain insight into the mutations contributing to melanocytic transformation by Lkb1 loss and UVB-induced melanomagenesis, we performed WES of eight tumors generated from different genetic backgrounds (three spontaneous (one $Braf^{CA/CA}$ (hereafter B) and two $Braf^{CA/+}$; $Lkb1^{-/-}$ (thereafter B;L)) and five UVB-induced tumors (three $Braf^{CA/+}$ and two $Braf^{CA/+}$; $Lkb1^{-/-}$)). We identified 1149 unique mutated genes among all analyzed mouse tumor samples (variant allele frequency; VAF > 10%; Table S1). Analysis of the cutaneous melanoma TCGA database (PanCancer) revealed 966 unique genes mutated in human samples (VAF > 10%; Table S1). One hundred and seventy-seven of these mutated genes, including Braf and

Stk11 (Lkb1), were identified in mouse and human melanomas. Gene set enrichment analysis revealed that these commonly mutated genes were associated with dysregulated tumor processes, including neural development (dedifferentiation), immune regulation, adhesion, motility, and signal transduction (Fig. 5A and Table S2). Mutational landscape analysis revealed that C>T transitions were the most frequent nucleotide substitutions in B + UVB and B;L + UVB tumors (62.8%) and 68.6%, respectively), while G>T transversions occurred more frequently in B;L tumors (77.5%) (Fig. 5B). All tumor types exhibited similar frequencies of alterations (the most frequent nonsynonymous variants), except for stop gains, which were more frequent in UVB-induced melanomas (Fig. 5C). The identified mutations targeted several protein family subtypes at different frequencies, although B;L + UVB tumors showed an increased mutation frequency in protein kinases and transcription factors (Fig. 5D). Then, we investigated which processes were affected by the identified mutated genes according to genotype and treatment. Despite the low number of tumors per group of analysis, genes mutated in UVB-irradiated tumors (VAF > 20%) were significantly associated with cancer-related biological processes such as extracellular matrix organization, adhesion, and motility, (Itga2b, Thbs4, Tnc, Itgal, Col6a5, Serpine1, Ptpn11, Cib1, and Ift74), including the activation of RHO signaling (Lmnb1, Myh9, Sh3bp1, Tuba3a, Zap70, Tiam2, Racgap1, Ndufs3, Rhobtb1, Dnmbp, Arhgef6, Dock8, Cenpi, Dock10, Fam91a1, Pde5a, Stard13, and Iggap2), which is involved in cytoskeletal dynamics and cell movement and is associated with mTORC2 activation [34,35]. Gene set enrichment analysis of the mutated genes in non-UVB-irradiated Lkb1-deficient tumors revealed associations with processes related to neurallike dedifferentiation (Neurod6, Cttn, Dmd, Mark2, Hsp90ab1, Kif5a, Lamb2, Matn2, Thbs4, Tulp1, Gprin1, Cntnap1, Camsap2, Nrn1, Actl6b, Bbs4, Unc5b,

18780261, 0, Downloaded from https://febs.onlinelibrary.wiley.com/doi/10.1002/1878-0261.13715 by Spanish Cochrane National Provision

de Sanidad), Wiley Online Library on [30/01/2025]. See the Terms

on Wiley Online Library for rules of use; OA articles are governed by the applicable Creative Commons

Fig. 5. Exome-sequencing mutational analysis. (A) Venn diagram showing the common unique mutated genes identified in the mouse model (VAF > 10%) and human samples (TCGA, Firehorse database) (VAF > 10%). The biological processes, associated to the identified mutated common genes (Metascape analysis) are shown on the right. (B) Percentage of transitions and transversions detected in each genotype [one $Braf^{CA/CA}$ (C), two $Braf^{CA/+};Lkb1^{-/-}$ (B;L), and five UVB-induced tumors (three $Braf^{CA/+}$ and two $Braf^{CA/+};Lkb1^{-/-}$)]. (C) Percentage of different types of genetic alterations found in the indicated genotypes and treatments. (D) Percentage of mutated genes belonging to the indicated groups of proteins. (E) Gene set enrichment analysis of the mutated genes with a variant allele frequency (VAF) > 10% showing the biological processes and pathways altered. (F) Percentage of mutated genes in each subtype of melanoma cells is described in Tsoi et al. [36].

Mcf2, Ntng2, Rnf165, Camsap1, Lrp4, Szt2, Gdf7, Nes, Plec, and Fat4), adhesion, motility, and dysregulation of the RHO signaling pathway (Atp6ap1, Cdc42ep3, Arhgap31, Mcf2, Fmnl3, Plekhg6, Ptpn13, Pkp4, Armcx3, and Baiap2l2) (Fig. 5E). Additionally, oncogene gene set analysis revealed that B;L tumors harbored mutations in genes associated with p53 (Crim1, Mark2, Dmd, Amb2, Unc13b, Msln, and Psmb8), mTOR (Adgre5, Cldn14, Irf7, Itpka, Alox15, and Ptprd), and PTEN (Fst, Nrn1, Pdzk1, Cldn14, Slc6a, Slc26a4, Tgfbr3, Kcnh7, and Lamc3) activity. Additionally, genes mutated in UVB-irradiated B;L tumors were significantly involved in neural differentiation (i.e., Col3a1, Col5a1, Enah, Ncam1, Sema4d, Dpysl3, Arhgef7, Sptbn4, Ptk2b, Trpc5, Rorb, Nyap, and Pak4) and altered genes involved in signal transduction (Egr4, Grid2, Fosb, Dyrk1b, Ror2, Prdm1, Ptk2b, Mapk10, Csf3r, Hras, Stat4, Six4, Rgs14, Grap, Pak4 Wnk2, Mapkbp1, and Arhgef7) and immunemodulating processes (Cav1, Ifnb1 Stat4, and Il23r) (Fig. 5E). Furthermore, these results were supported by the percentage of mutated genes belonging to the different signatures defining the melanoma cell subtypes [36] (Fig. 5F and Table S2). Taken together, these results support the cooperation of Lkb1 loss with Braf^{V600E} in melanoma development and its association with morphological neural-like dedifferentiation.

4. Discussion

The signaling pathways that cooperate with MAP-K/ERK activation in $BRAF^{V600E}$ melanoma are of great interest. Several studies have demonstrated that UVR can cooperate with the $BRAF^{V600E}$ mutation, bypassing oncogene-induced cell cycle arrest and promoting uncontrolled cell proliferation and tumor development [8,9]. In addition, Pten or NfI loss abrogates $Braf^{V600E}$ -induced oncogene-induced senescence (OIS) and leads to $in\ vivo$ melanoma formation and LkbI loss abrogates $Braf^{V600E}$ -induced cell growth arrest without full progression to malignancy [10,11,37]. Despite the well-known functions of LKB1 as a tumor suppressor, LKB1 also plays a relevant role

in DDR [12-15], suggesting cooperation among $BRAF^{V600E}$ mutations, UVR-induced DNA damage, and/or LKB1 loss to promote melanomagenesis.

Initial analysis of human samples from the TCGA database supported previous observations suggesting low expression or inactivation of LKB1 in melanoma patients [22,23]. These data also revealed a negative correlation between BRAF and STK11 mRNA and protein expression. While many patients suffer shallow copy number deletions in the STK11 gene, the BRAF locus is subjected to copy number gains or amplifications. However, STK11 mRNA was more abundant than BRAF mRNA, which could be interpreted as a compensatory mechanism at the transcriptional level that did not correlate with the corresponding amount of protein expression. This negative correlation of BRAF and STK11 at the protein level was also observed in our validation subset of BRAFV600Emutated human melanomas, supporting the notion of a lack of expression or low amounts of LKB1 in at least 50% of BRAF^{V600E}-mutated samples. Due to this observation and the role of LKB1 in DNA damage repair [12-15], we investigated the contributions of Lkb1 loss to UVR-induced melanoma development and progression in a Braf W600E mutational context. In contrast to a previous report [27], Lkb1 haploinsufficiency cooperated with BrafV600E, promoting full tumorigenesis, although progression occurred at a longer time than previously reported. Further characterization of these tumors by immunohistochemistry also confirmed the activation of both mTORC1 and mTORC2/Akt pathways for cell progression to malignancy [27]. Lkb1 loss did not further increase Braf V600E UVR-induced melanoma, probably due to the high tumor penetrance in the model. For unknown reasons currently under investigation, the loss of both Lkb1 alleles $(Lkb1^{-/-})$ promoted a delay in melanoma development. However, in agreement with the impaired UVB-induced DNA damage repair and the described role of LKB1 in DDR, the loss of $Lkb1^{-/-}$ contributed to genetic instability, increasing tumor multiplicity, even compared with that in heterozygous mice $(Lkb1^{+/-})$. These data also support the

acquisition of additional genetic alterations in the absence of UVB radiation, which will facilitate the promotion of full tumorigenesis in Braf^{V600E} melanocytes upon Lkb1 loss. Nevertheless, in irradiated Braf^{CA};Lkb1^{-/-} melanocytes, tumor cells adaptation and evolution (i.e., metabolic rewiring and/or DNA damage repair in the absence of LKB1) to this complex mutational landscape might be one of the causes behind delay in tumor development observed in these mice.

Although three major histological morphologies were identified in most of the samples, melanomas with neural-like differentiation were more frequent upon Lkb1 deletion. Tumor morphological heterogeneity increases upon Lkb1 loss, coincident with the genetic instability generated by an impaired DDR [12,13,38]. It is documented that LKB1 governs the formation and maintenance of several neural crest derivatives, including melanocytes [30,39]. Additionally, melanoma is known to exhibit phenotypic plasticity and trans-differentiation along vascular and neural lineages [40]. The enrichment in neural-like morphology in Lkb1-deficient tumors, including UV-irradiated tumors, suggested a differential melanocyte subtype for tumor origin. This hypothesis was supported by the observed differential expression of LKB1 in melanocytes at 7 days postnatally, and previous reports showing that melanoma can arise from either melanocyte stem cells or differentiated melanocytes depending on the tissue and anatomical site of origin, activation of oncogenic mutations, and/or the or inactivating mutations in tumor suppressors [40]. Our experiments do not distinguish whether LKB1 expression is something transiently related to melanocyte biology, or it is a permanent feature of certain melanocytes within the hair follicle. However, this result suggests that there will be melanocytes particularly affected by the loss of LKB1 (transiently or permanently).

The mutational profiling of mouse tumor samples revealed that 10% of the identified genes were also mutated in human samples, revealing a similar number of unique mutated genes supporting the relevance of the mouse model. In the UVB-irradiated samples, C-to-T transitions accumulated, while in the nonirradiated samples, G-to-T transversions accumulated, indicating the participation of alternative mutational mechanisms mostly in the absence of Lkb1. Nonsynonymous variants were the predominant type of mutation, and stop gains accumulated, especially in the irradiated samples. There was a slight increase in nonframeshift deletions in the nonirradiated Lkb1-null samples, which also revealed differences in the frequencies of mutated genes in the protein families. The guanine base (G) in genomic DNA is highly susceptible to oxidative stress due to having the lowest oxidation potential. Therefore, $G \cdot C \rightarrow$ $T \cdot A$ and $G \cdot C \rightarrow C \cdot G$ transversion mutations frequently occur under oxidative conditions [41]. LKB1 deficiency increases the sensitivity of cells to radiation-induced carcinogenesis and ROS, resulting in excessive DNA oxidation and mutation [13,42], affecting genomic stability in several ways, and contributing to cancer development [43]. In this matter, Lkb1 inactivation, particularly in melanocytes, where melanin production yields high amounts of hydrogen peroxide, would contribute to DNA damage reflected in the type of point mutations identified in Lkb1 null tumors. In fact, we have observed that Lkb1^{-/-}-deficient tumors, independently of UVB radiation, harbored an average of fourfold more mutations than Braf^{CA} tumors (data not showed). This piece of data agrees with the elevated tumor mutational burden (TMB) observed in NSCLCs from nonsmokers and mouse models upon LKB1 deficiency [44].

The comprehensive analysis (Metascape) of the mutated gene lists according to the mouse genotype and treatment indicated that Braf V600E tumors showed alterations in motility, adhesion, and cell signaling processes. Interestingly, Lkb1-null tumors, independent of UVB radiation status, showed a clear enrichment of neural differentiation-related processes, supporting the dedifferentiation and predominant neural-like morphology linked to those tumors. These data are in line with the role of LKB1 signaling in neural development and homeostasis [45], and the development of neural crest cell derivatives such as melanocytes [30]. Furthermore. due to the pleiotropic roles of LKB1 in cancer (i.e., cell viability, invasiveness, and metabolism), the dysregulation of all these distinct aspects will also contribute to mutation landscape selection and malignancy.

5. Conclusion

Overall, this study and our previous reports [12,29,46,47] identified the loss of LKB1 as an important mechanism alongside the BRAFV600E mutation in cancer development and progression. The loss of the multitask LKB1 kinase contributes to melanoma development through dysregulation of multiple processes, including an increase in genomic instability caused by a deficient DDR. Loss of LKB1 not only makes cells especially vulnerable to UVB radiation and prone to oncogenes and/or tumor suppressors but also promotes melanocyte transformation toward a neural-like phenotype. Thus, we identified the loss of LKB1 as a mechanism alongside BRAF V600E and UVB that contributes melanocyte transformation melanomagenesis.

onlinelibrary.wiley.com/doi/10.1002/1878-0261.13715 by Spanish Cochrane National Provision (Ministerio de Sanidad), Wiley Online Library on [30/01/2025]. See the Terms conditions) on Wiley Online Library for rules of use; OA articles are governed by the applicable Creative Commons

Acknowledgements

This work was funded by Instituto de Salud Carlos III and co-funded by the European Union (ERDF/ESF, "A way to make Europe"/"Investing in your future"), PI17/00043-Fondos FEDER; PI20/0384-Fondos FEDER; PI23/00428-Fondos FEDER JAR, Institute of Health Carlos III-Euronanomed-II (AC16/00019)-Fondos FEDER European Union; and JAR, Asociación Española Contra el Cancer (AECC-GCB15152978SOEN). AGAUR, 2021-SGR00653 JAR (supported PG-M, KM); Ramón Areces Foundation (supported KM and research); JAR.

Conflict of interest

The authors declare no conflict of interest.

Author contributions

JAR and KM contributed to conceptualization. KM, PG-M, RO, YD, EG-S, BF, JH-L, IO, JM-C, and JAR contributed to investigation. JAR, VG-P, andEM-C contributed to resources. JAR and VG-P contributed to funding acquisition. KM, PG-M, IO, and YD contributed to methodology. JAR, BF, VG-P, EM-C, and KM contributed to formal analysis. JAR and KM contributed to writing—review and editing. JAR contributed to supervision.

Peer review

The peer review history for this article is available at https://www.webofscience.com/api/gateway/wos/peerreview/10.1002/1878-0261.13715.

Data accessibility

The gene alteration data used in this study are publicly available at cBioPortal (Skin Cutaneous Melanoma; TCGA, PanCancer Atlas, 448 samples; https://www.cbioportal.org). The exome-sequencing datasets reported in this article have been deposited in the National Center for Biotechnology Information (NIH) under accession number PRJNA1073850.

References

- Davies H, Bignell GR, Cox C, Stephens P, Edkins S, Clegg S, et al. Mutations of the BRAF gene in human cancer. *Nature*. 2002;417:949–54.
- 2 Greaves WO, Verma S, Patel KP, Davies MA, Barkoh BA, Galbincea JM, et al. Frequency and spectrum of

- BRAF mutations in a retrospective, single-institution study of 1112 cases of melanoma. *J Mol Diagn*. 2013:**15**:220–6.
- 3 Long GV, Menzies AM, Nagrial AM, Haydu LE, Hamilton AL, Mann GJ, et al. Prognostic and clinicopathologic associations of oncogenic BRAF in metastatic melanoma. *J Clin Oncol.* 2011;**29**:1239–46.
- 4 Pollock PM, Harper UL, Hansen KS, Yudt LM, Stark M, Robbins CM, et al. High frequency of BRAF mutations in nevi. *Nat Genet*. 2003;33:19–20.
- 5 Michaloglou C, Vredeveld LCW, Soengas MS, Denoyelle C, Kuilman T, van der Horst CMAM, et al. BRAFE600-associated senescence-like cell cycle arrest of human naevi. *Nature*. 2005;436:720–4.
- 6 Armstrong BK, Kricker A. The epidemiology of UV induced skin cancer. *J Photochem Photobiol B*. 2001:63:8–18.
- 7 Noonan FP, Recio JA, Takayama H, Duray P, Anver MR, Rush WL, et al. Neonatal sunburn and melanoma in mice. *Nature*. 2001;**413**:271–2.
- 8 Luo C, Sheng J, Hu MG, Haluska FG, Cui R, Xu Z, et al. Loss of ARF sensitizes transgenic BRAFV600E mice to UV-induced melanoma via suppression of XPC. *Cancer Res.* 2013;73:4337–48.
- 9 Viros A, Sanchez-Laorden B, Pedersen M, Furney SJ, Rae J, Hogan K, et al. Ultraviolet radiation accelerates BRAF-driven melanomagenesis by targeting TP53. *Nature*. 2014:**511**:478–82.
- 10 Dankort D, Curley DP, Cartlidge RA, Nelson B, Karnezis AN, Damsky WE Jr, et al. Braf(V600E) cooperates with Pten loss to induce metastatic melanoma. *Nat Genet*. 2009;41:544–52.
- 11 Gibney GT, Smalley KS. An unholy alliance: cooperation between BRAF and NF1 in melanoma development and BRAF inhibitor resistance. *Cancer Discov.* 2013;3:260–3.
- 12 Esteve-Puig R, Gil R, González-Sánchez E, Bech-Serra JJ, Grueso J, Hernández-Losa J, et al. A mouse model uncovers LKB1 as an UVB-induced DNA damage sensor mediating CDKN1A (p21WAF1/CIP1) degradation. *PLoS Genet*. 2014;10:e1004721.
- 13 Gupta R, Liu AY, Glazer PM, Wajapeyee N. LKB1 preserves genome integrity by stimulating BRCA1 expression. *Nucleic Acids Res.* 2015;**43**:259–71.
- 14 Ui A, Ogiwara H, Nakajima S, Kanno S, Watanabe R, Harata M, et al. Possible involvement of LKB1-AMPK signaling in non-homologous end joining. *Oncogene*. 2014;33:1640–8.
- 15 Wang YS, Chen J, Cui F, Wang H, Wang S, Hang W, et al. LKB1 is a DNA damage response protein that regulates cellular sensitivity to PARP inhibitors. Oncotarget. 2016;7:73389–401.
- 16 Ji H, Ramsey MR, Hayes DN, Fan C, McNamara K, Kozlowski P, et al. LKB1 modulates lung cancer differentiation and metastasis. *Nature*. 2007;448:807–10.

onlinelibrary.wiley.com/doi/10.1002/1878-0261.13715 by Spanish Coch de Sanidad), Wiley Online Library on [30/01/2025]. See the Terms on Wiley Online Library for rules of use; OA articles are governed by the applicable Creative Commons

- 17 Sanchez-Cespedes M, Parrella P, Esteller M, Nomoto S, Trink B, Engles JM, et al. Inactivation of LKB1/STK11 is a common event in adenocarcinomas of the lung. *Cancer Res.* 2002;**62**:3659–62.
- 18 McCabe MT, Powell DR, Zhou W, Vertino PM. Homozygous deletion of the STK11/LKB1 locus and the generation of novel fusion transcripts in cervical cancer cells. *Cancer Genet Cytogenet*. 2010;197:130–41.
- 19 Morton JP, Jamieson NB, Karim SA, Athineos D, Ridgway RA, Nixon C, et al. LKB1 haploinsufficiency cooperates with Kras to promote pancreatic cancer through suppression of p21-dependent growth arrest. *Gastroenterology*. 2010;**139**:586–97, e1–6.
- 20 Su GH, Hruban RH, Bansal RK, Bova GS, Tang DJ, Shekher MC, et al. Germline and somatic mutations of the STK11/LKB1 Peutz-Jeghers gene in pancreatic and biliary cancers. *Am J Pathol*. 1999;154:1835–40.
- 21 Shen Z, Wen XF, Lan F, Shen ZZ, Shao ZM. The tumor suppressor gene LKB1 is associated with prognosis in human breast carcinoma. *Clin Cancer Res.* 2002:**8**:2085–90.
- 22 Guldberg P, thor Straten P, Ahrenkiel V, Seremet T, Kirkin AF, Zeuthen J. Somatic mutation of the Peutz-Jeghers syndrome gene, LKB1/STK11, in malignant melanoma. *Oncogene*. 1999;18:1777–80.
- 23 Rowan A, Bataille V, MacKie R, Healy E, Bicknell D, Bodmer W, et al. Somatic mutations in the Peutz-Jeghers (LKB1/STKII) gene in sporadic malignant melanomas. *J Invest Dermatol*. 1999;112:509–11.
- 24 Giardiello FM, Brensinger JD, Tersmette AC, Goodman SN, Petersen GM, Booker SV, et al. Very high risk of cancer in familial Peutz-Jeghers syndrome. *Gastroenterology*. 2000;**119**:1447–53.
- 25 Lim W, Olschwang S, Keller JJ, Westerman AM, Menko FH, Boardman LA, et al. Relative frequency and morphology of cancers in STK11 mutation carriers. *Gastroenterology*. 2004;126:1788–94.
- 26 Liu W, Monahan KB, Pfefferle AD, Shimamura T, Sorrentino J, Chan KT, et al. LKB1/STK11 inactivation leads to expansion of a prometastatic tumor subpopulation in melanoma. *Cancer Cell*. 2012;21:751–64.
- 27 Damsky W, Micevic G, Meeth K, Muthusamy V, Curley DP, Santhanakrishnan M, et al. mTORC1 activation blocks BrafV600E-induced growth arrest but is insufficient for melanoma formation. *Cancer Cell*. 2015;27:41–56.
- 28 Gurumurthy S, Hezel AF, Sahin E, Berger JH, Bosenberg MW, Bardeesy N. LKB1 deficiency sensitizes mice to carcinogen-induced tumorigenesis. *Cancer Res*. 2008;68:55–63.
- 29 Gonzalez-Sanchez E, Martín-Caballero J, Flores JM, Hernández-Losa J, Montero MA, Cortés J, et al. Lkbl loss promotes tumor progression of BRAF(V600E)induced lung adenomas. *PLoS One*. 2013;8:e66933.

- 30 Radu AG, Torch S, Fauvelle F, Pernet-Gallay K, Lucas A, Blervaque R, et al. LKB1 specifies neural crest cell fates through pyruvate-alanine cycling. *Sci Adv.* 2019;**5**:eaau5106.
- 31 Dankort D, Filenova E, Collado M, Serrano M, Jones K, McMahon M. A new mouse model to explore the initiation, progression, and therapy of BRAFV600E-induced lung tumors. *Genes Dev.* 2007;21:379–84.
- 32 Recio JA, Noonan FP, Takayama H, Anver MR, Duray P, Rush WL, et al. Ink4a/arf deficiency promotes ultraviolet radiation-induced melanomagenesis. *Cancer Res.* 2002;**62**:6724–30.
- 33 Tosti A, Cameli N, Piraccini BM, Fanti PA, Ortonne JP. Characterization of nail matrix melanocytes with anti-PEP1, anti-PEP8, TMH-1, and HMB-45 antibodies. *J Am Acad Dermatol*. 1994;31(2 Pt 1):193–6. https://doi.org/10.1016/s0190-9622(94)70144-x
- 34 Li X, Gao T. mTORC2 phosphorylates protein kinase Czeta to regulate its stability and activity. *EMBO Rep.* 2014;15:191–8.
- 35 Senoo H, Kamimura Y, Kimura R, Nakajima A, Sawai S, Sesaki H, et al. Phosphorylated Rho-GDP directly activates mTORC2 kinase towards AKT through dimerization with Ras-GTP to regulate cell migration. *Nat Cell Biol.* 2019;**21**:867–78.
- 36 Tsoi J, Robert L, Paraiso K, Galvan C, Sheu KM, Lay J, et al. Multi-stage differentiation defines melanoma subtypes with differential vulnerability to drug-induced iron-dependent oxidative stress. *Cancer Cell*. 2018;33:890–904.e5.
- 37 Vredeveld LC, Possik PA, Smit MA, Meissl K, Michaloglou C, Horlings HM, et al. Abrogation of BRAFV600E-induced senescence by PI3K pathway activation contributes to melanomagenesis. *Genes Dev.* 2012;26:1055–69.
- 38 Jin LY, Zhao K, Xu LJ, Zhao RX, Werle KD, Wang Y, et al. LKB1 inactivation leads to centromere defects and genome instability via p53-dependent upregulation of survivin. *Aging (Albany NY)*. 2020;12:14341–54.
- 39 Thibert C, Lucas A, Billaud M, Torch S, Mevel-Aliset M, Allard J. Functions of LKB1 in neural crest development: the story unfolds. *Dev Dyn*. 2023;252:1077–95.
- 40 Castro-Perez E, Singh M, Sadangi S, Mela-Sanchez C, Setaluri V. Connecting the dots: melanoma cell of origin, tumor cell plasticity, trans-differentiation, and drug resistance. *Pigment Cell Melanoma Res*. 2023;36:330–47.
- 41 Kino K, Sugiyama H. Possible cause of G-C-->C-G transversion mutation by guanine oxidation product, imidazolone. *Chem Biol*. 2001;8:369–78.
- 42 Xu HG, Zhai YX, Chen J, Lu Y, Wang JW, Quan CS, et al. LKB1 reduces ROS-mediated cell damage via activation of p38. *Oncogene*. 2015;34:3848–59.

- 43 Li TT, Zhu HB. LKB1 and cancer: the dual role of metabolic regulation. *Biomed Pharmacother*. 2020;132:110872.
- 44 Deng J, Thennavan A, Dolgalev I, Chen T, Li J, Marzio A, et al. ULK1 inhibition overcomes compromised antigen presentation and restores antitumor immunity in LKB1 mutant lung cancer. *Nat Cancer*, 2021;2:503–14.
- 45 Kuwako KI, Okano H. Versatile roles of LKB1 kinase signaling in neural development and homeostasis. *Front Mol Neurosci.* 2018;**11**:354.
- 46 Esteve-Puig R, Canals F, Colome N, Merlino G, Recio JA. Uncoupling of the LKB1-AMPKalpha energy sensor pathway by growth factors and oncogenic BRAF. *PLoS One*. 2009;4:e4771.

47 Granado-Martinez P, Garcia-Ortega S, González-Sánchez E, McGrail K, Selgas R, Grueso J, et al. STK11 (LKB1) missense somatic mutant isoforms promote tumor growth, motility and inflammation. *Commun Biol.* 2020;3:366.

Supporting information

Additional supporting information may be found online in the Supporting Information section at the end of the article.

Table S1. List of unique mutated genes in mouse and human samples.

Table S2. Melanoma subtype gene signatures.